

# A Facile Strategy To Prepare Smart Coatings with Autonomous Self-Healing and Self-Reporting Functions

Shusheng Chen, Ting Han, Ying Zhao, Wenjun Luo, Zhong Zhang, Haibin Su, Ben Zhong Tang,\* and Jinglei Yang\*

Cite This: *ACS Appl. Mater. Interfaces* 2020, 12, 4870–4877

Read Online

ACCESS |

Metrics & More

Article Recommendations

Supporting Information

**ABSTRACT:** Herein, we report a smart coating with autonomous self-healing and self-reporting functions by simple integration of one-component microcapsules into the matrix without external intervention. The microcapsules containing hexamethylene diisocyanate (HDI) solution of aggregation-induced emission luminogens (AIEgens) were synthesized, and their properties, such as their composition, thermal stability, morphology, and damage-indicating ability, were investigated systematically. The AIEgen/HDI microcapsule-embedded coatings display adaptive self-repair of scratches and simultaneous high-contrast indication of the healed damage. Two commercialized AIEgens, tetraphenylethylene (TPE) and its derivative with dimethoxyl and benzylidene-methyloxazolone moieties (DM-TPE-BMO), were utilized as examples to demonstrate the feasibility of this concept in diverse polymer matrixes (including blue autofluorescent matrixes). It was found that the content of AIEgens can even be lowered to 0.05 wt %. This facile, economical, and feasible strategy toward the dual functions of self-repairing and self-sensing provides a new route for enhancing the longevity and reliability of polymer coatings, which is appealing and of great importance in practical applications.

**KEYWORDS:** self-healing, self-reporting, polymer coating, microcapsule, aggregation-induced emission luminogens

## 1. INTRODUCTION

Living organisms are able to not only self-recover from injuries but also self-report the damaged area to guide external spot-repair processes and prevent further damage to the same site. Taking human skin as an example, it is capable of reporting the injuries by bruising or bleeding and autonomously self-healing the wounds in the meantime. Inspired by nature, scientists have made remarkable progress in microcapsule-based self-healing polymers with broad applications in polymer coatings and composites during the past decades.<sup>1–4</sup> A wide variety of healing agents, such as dicyclopentadiene,<sup>5</sup> epoxy,<sup>6</sup> amine,<sup>7</sup> thiol,<sup>8</sup> glycidyl methacrylate,<sup>9</sup> and isocyanate,<sup>10</sup> have been successfully microencapsulated for different types of self-healing systems including single-capsule systems, capsule/dispersed catalyst systems, double-capsule systems, and all-in-one microcapsule systems.<sup>11</sup> In addition to self-healing, researchers have also investigated microcapsule-based polymers with mechanochromic or self-reporting capability. It is a simple and versatile concept to achieve the self-sensing ability using microcapsules containing solutions of dyes that are released and physically or chemically activated when the microcapsules are ruptured.<sup>12</sup> The current reports on self-reporting composites based on microcapsules could be classified into three principles, namely, simple release of an encapsulated dye,<sup>13–15</sup> turn-on mechanism based on interactions of a cargo and its matrix<sup>16–19</sup> or payloads from two separate reservoirs,<sup>20,21</sup> and physically aggregation-

induced optical changes.<sup>22–25</sup> Although research efforts on self-healing or self-reporting single-function materials have witnessed significant growth, to the best of our knowledge, only a few smart biomimetic polymers with dual functions of self-healing and self-reporting based on the encapsulation concept have been explored.

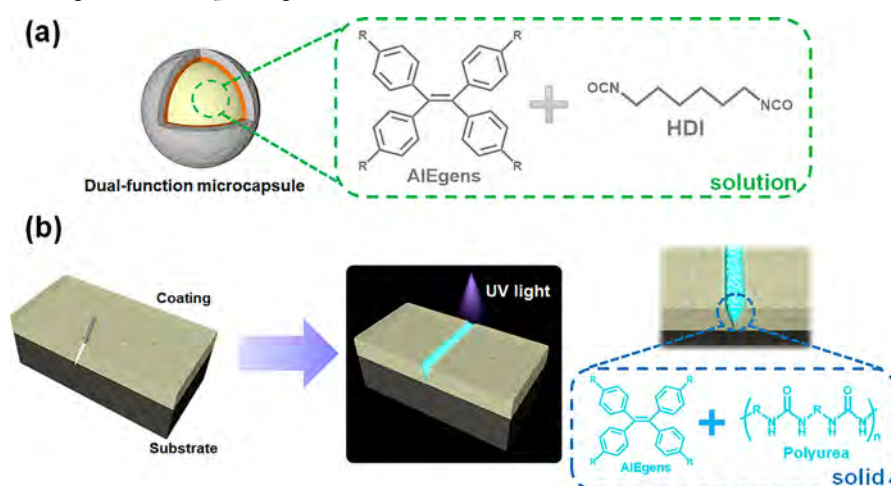
Zhang et al.<sup>26</sup> investigated a fully automatic dual-function composite by incorporating double microcapsules containing epoxy dyed with a pH indicator and polyamine as a multirole trigger. The self-repairing function was triggered by the reaction between the epoxy and polyamine. The self-warning capacity was activated when the pH indicator was in contact with polyamine. Wang et al.<sup>27</sup> synthesized pH-responsive and porous microspheres that separately contained a corrosion inhibitor and a fluorescent probe. The polymer coating embedded with these two microspheres can adapt to the variation in pH value from the electrochemical corrosion and release active molecules into the damaged regions, leading to the dual functions of self-healing and self-reporting. Hu et al.<sup>28</sup> designed a single-nanocapsule in which an inactive dye, crystal violet lactone (CVL), was

**Received:** October 19, 2019

**Accepted:** December 30, 2019

**Published:** December 30, 2019

**Scheme 1.** (a) Schematic Diagram of a One-Part Microcapsule Containing HDI Solution of AIEgens; (b) Schematic Description of Autonomous Self-Healing and Self-Reporting Dual Functions



encapsulated by a polymer shell coated with a color developer. When capsules were mechanically broken, the colorless CVL transferred to a colored form by reacting with the color developer. Taking advantage of the reversible reaction between CVL and color developers, the author manually added healing agents into damaged areas, which can “turn off” the damage detection after healing, thus allowing the tracing of the self-sensing and repairing cycle. Song et al.<sup>29</sup> reported a single-capsule system, the core of which comprised photocuring healing agents and tetraphenylethylene (TPE) as an indicator. The microcapsules and epoxy resin were mixed to form a dual-function coating covered with a UV-screening top coating. The self-healing ability was achieved with the aid of external UV illumination and blue fluorescence was observed at the healed regions after the photocuring process because of the aggregation-induced emission (AIE). The same group then mixed the epoxy matrix with a yellow light-emitting dye to detect both damaged and healed states of the dual-function coating.<sup>30</sup> The above topics of research are double-capsule systems that contain a color indicator and healing agents in separate microcapsules or porous microspheres, and single-capsule systems that repair damage with the aid of extra UV treatment or manual addition of healant. However, there are limited reports on the warning of and healing damage without external intervention in one-component microcapsule-based materials.

In the present work, we develop a facile strategy to prepare smart anticorrosion coatings with double functions of in situ or autonomous self-healing and self-reporting. This is achieved by simply embedding one-part, dual-function microcapsules containing hexamethylene diisocyanate (HDI) and AIE luminogens (AIEgens) in the polymer coatings. HDI, which can automatically react with water, is one of the most promising one-component and catalyst-free self-healing agents.<sup>31–33</sup> AIEgens are robust turn-on damage-detecting agents owing to the unique AIE characteristic. In our case, HDI functions as both the solvent of AIEgens and the healant of the polymer coatings.

## 2. EXPERIMENTAL DETAILS

**2.1. Experimental Design.** As illustrated in Scheme 1, microcapsules containing HDI solution of AIEgens without any other organic solvents were prepared and embedded into a polymer coating. When the microcapsules were subjected to mechanical damage, they ruptured, leading to the release of their payload in the damaged regions.

Subsequent spontaneous reaction between HDI and water formed polyurea (PU) solid materials, which then filled and healed the cracks automatically. At the same time, the scratched and healed areas became strongly fluorescent because of the restriction and aggregation of AIEgens in these areas.<sup>25</sup> The fluorescence of AIEgens can be clearly visualized under UV illumination and thus can be utilized as an indicator to report the damaged sites.

**2.2. Materials.** 4,4-Diphenylmethane diisocyanate (MDI) prepolymer Suprasec 2644 was obtained from Huntsman. Hexamethylene diisocyanate (HDI), Gum Arabic, formaldehyde solution (37 wt %), urea, resorcinol, polyethylenimine (PEI,  $M_n \sim 1800$ , 50 wt % aqueous solution), poly(ethylene-*alt*-maleic anhydride) (EMA,  $M_w$  100 000–500 000), sodium hydroxide (NaOH), sodium chloride (NaCl), and tetrahydrofuran (THF) were purchased from Sigma-Aldrich. Tetraphenylethylene (TPE) was purchased from Energy Chemical. The TPE derivative with dimethoxyl and benzylidene-methyloxazolone moieties (DM-TPE-BMO) was obtained from AIEgen Biotech Co. Limited. Steel panels were purchased from Haoxun Steel Company. Epolam 5015 epoxy resin and its hardener 5015 were supplied by Axson. Sikafloor 156 epoxy resin and its hardener were purchased from Sika Company. All chemical reagents were used as received and without further purification.

**2.3. Preparation of Microcapsules.** Double-layered microcapsules containing HDI solution of AIEgens were synthesized via a two-step method that included interfacial polymerization of polyurea (PU) and in situ polymerization of poly(urea-formaldehyde) (PUF).<sup>34,35</sup> For optimization of the microencapsulation process, the agitation rate for PU synthesis and the reaction duration for PUF synthesis were studied systematically and evaluated in terms of the size and core fraction of the resultant microcapsules. Typically, in the first step, the inner PU shells of the microcapsules were synthesized through interfacial polymerization. The oil-phase mixture of 2 g of Suprasec 2644 and 8 g of AIEgen/HDI solution (0.5 wt % of TPE or 0.05 wt % of DM-TPE-BMO) was added dropwise into 60 mL of gum arabic aqueous solution (3 wt %) under an agitation rate of 1000 rpm (Cafraimo, model: BDC6015) for 15 min followed by the addition of 2 g of PEI to initiate interfacial polymerization. The reaction temperature was raised to 40 °C. After 4 h, the PU microcapsules were decanted and rinsed with deionized water several times. In the subsequent step, PUF shells were deposited on the microcapsules by in situ polymerization. UF prepolymer was first prepared by the reaction of 12.66 g of formaldehyde solution and 6 g of urea under a pH of 8 at 70 °C for 1 h. The PU microcapsules were mixed with UF prepolymer and 5 g of resorcinol in 60 mL of EMA aqueous solution (2.5 wt %) before adjusting the pH of the mixture to 3. The system was left to react under an agitation rate of 200 rpm at 40 °C for 1 h. The final microcapsules containing AIEgens/HDI were rinsed with deionized water several

times and dried in air overnight. Following the procedures above, we prepared microcapsules containing HDI as references.

**2.4. Preparation of Self-Healing and Self-Reporting Coating.** Epoxy resin (Epilam 5015 or Sikafloor 156) was first mixed with its hardener before 10 wt % of microcapsules was added. After the mixture was degassed in a vacuum oven for 20 min, it was coated onto polished steel panels with the final thickness of 300–400  $\mu\text{m}$  and then completely cured at room temperature. Pure epoxy coatings were prepared following the same procedure as for the controls. After scratching the coatings with a razor blade, the corrosion process was conducted by immersing the cured specimens in NaCl aqueous solution (10 wt %) for 24 h.

**2.5. Characterization.** UV–vis spectra and photoluminescence (PL) spectra were obtained on a PerkinElmer Lambda 365 UV/vis spectrophotometer and a Horiba Fluorolog spectrophotometer, respectively. Fluorescence quantum yields ( $\Phi_F$ ) were measured by a Hamamatsu absolute photoluminescence quantum yield spectrometer C11347 Quantaaurus QY. AIEgens/HDI solutions containing 0.5 wt % of TPE or 0.05 wt % of DM-TPE-BMO were prepared for UV–vis, PL, and  $\Phi_F$  measurement before and after curing.

Fourier transform infrared (FTIR) spectra were recorded on a Bruker Vertex 70 FTIR spectrometer. Thermogravimetric analysis (TGA) was conducted under a nitrogen atmosphere with a TA Q5000 thermal analyzer from 25 to 800  $^{\circ}\text{C}$  at a heating rate of 20  $^{\circ}\text{C}/\text{min}$ . The core fractions of microcapsules were estimated from the isothermal TGA testing.<sup>34</sup> Specifically, the microcapsules were heated at a rate of 20  $^{\circ}\text{C}/\text{min}$  from 25 to 180  $^{\circ}\text{C}$  and then kept isothermal for 1 h before the samples were finally heated to 800  $^{\circ}\text{C}$  in nitrogen. At least three samples were prepared using the same parameters and then each sample was tested, from which the mean value and standard deviation were derived. Pure capsule shells used for FTIR and TGA analysis were obtained by crushing a small number of microcapsules and then washing by ethanol several times.

Scanning electron microscopy (JEOL-6390) was applied to observe the morphologies of the microcapsules and scratched areas of coatings. The mean diameter of the microcapsules and their size distribution were measured and analyzed from SEM images of at least 200 measurements using ImageJ. Microcapsules were mounted on conductive tape and some of them were ruptured with a razor blade to observe the core–shell structure. All samples of microcapsules and coatings were coated with a thin layer of gold before SEM observation.

Photographic and stereomicroscopic images of microcapsules and scratched areas of coatings were respectively acquired using a digital camera (Canon EOS 60D) and microscope (Motic Moticam 1080) under ambient room lighting and illumination with a hand-held UV lamp (Spectroline ENF-260C). Microcapsules were spread on a glass slide and half of them were manually damaged to evaluate their damage-reporting ability.

### 3. RESULTS AND DISCUSSION

**3.1. Reactivity and Characterization of AIEgens/HDI Solution.** To demonstrate the design concept shown in Scheme 1, tetraphenylethylene (TPE) was chosen as the representative AIEgen because of its wide commercial availability. As shown in Figure 1a, pure HDI and TPE/HDI solution (0.5 wt %) were cured with water to form pure polyurea (PU) and TPE/PU solid, respectively. The absorption spectrum of TPE in HDI solution is similar to that in a common organic solvent (THF), showing a wavelength of maximum absorption at 320 nm (Figure S1, Supporting Information). Under the illumination of UV light, the HDI solutions and PU solid are almost nonemissive, whereas distinct blue fluorescence is observed for the TPE/PU solid. These results suggest the HDI and PU background has little interference on the absorption and fluorescence of TPE. We then measured the PL spectrum and  $\Phi_F$  of TPE/HDI before and after curing with water. The emission of TPE/HDI solution is too weak to be detected by the

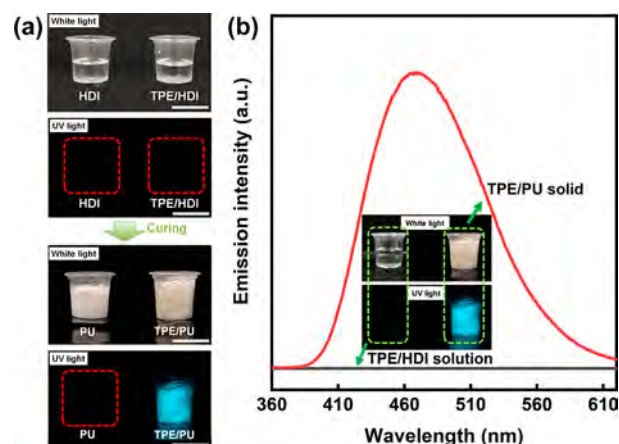


**Figure 1.** (a) Photographs of pure HDI solution, TPE/HDI solution, pure PU solid, and TPE/PU solid taken under the illumination of white light and UV light, respectively. The white scale bar indicates 200 mm in all images. (b) PL spectra of the TPE/HDI solution and TPE/PU solid. Excitation wavelength: 320 nm. The insets are photographs of TPE/HDI solution and TPE/PU solid taken under the illumination of white light and UV light.

PL spectrophotometer. Once HDI is polymerized into PU, bright blue fluorescence of TPE can be observed with an emission peak at around 470 nm, which is similar to the PL behavior of pure TPE powder.<sup>36</sup> The  $\Phi_F$  value of the TPE/HDI system significantly increased from 1.0% (solution) to 25.1% (solid), which is in agreement with the AIE mechanism. All these results are indicative of the feasibility of our design strategy.

**3.2. Preparation and Characterization of AIEgens/HDI Microcapsules.** The core fractions of the microcapsules were calculated from the isothermal test results and the typical TGA curves are shown in Figure S2. As summarized in Tables S1 and S2 and Figure S3, the size and core fraction of the microcapsules gradually decreased as the agitation rate for PU synthesis or reaction duration for PUF synthesis increased. After comprehensive analysis, 1000 rpm of agitation rate and 1 h of the reaction time were chosen as the optimal parameters to prepare microcapsules with a mean diameter of 106  $\mu\text{m}$  and a core fraction of  $61.7 \pm 3.7$  wt % for this study.

The composition of the obtained microcapsules was analyzed using FTIR (Figure 2a). In the spectra of TPE/HDI and HDI microcapsules, the strong absorption peak at around 2270  $\text{cm}^{-1}$  is associated with the stretching vibration of  $-\text{N}=\text{C}=\text{O}$  group,<sup>31</sup> which is consistent with that of pure HDI. By comparison, no characteristic signal related to the  $-\text{N}=\text{C}=\text{O}$  stretching vibration is detected in the IR spectrum of the microcapsule shells, indicating that the MDI prepolymer was consumed to form the bulk shells of the microcapsules. These results suggested that the core of TPE/HDI and HDI were successfully encapsulated into the microcapsules. The absorption peaks at the range of 3000–3100 and 500–800  $\text{cm}^{-1}$  corresponding to aromatic C–H stretching and bending vibrations of TPE are hardly detected in the spectrum of TPE/HDI microcapsules, indicating that the concentration of TPE is too low to be detected by FTIR.

The thermal stability of microcapsules was investigated by TGA. Figure 2b shows that the naked HDI starts to evaporate at about 90  $^{\circ}\text{C}$ , whereas the initial decomposition temperature of TPE/HDI and HDI microcapsules is around 180  $^{\circ}\text{C}$ . These results indicate that the encapsulated HDI has better thermal stability than naked HDI. Such a great improvement results from



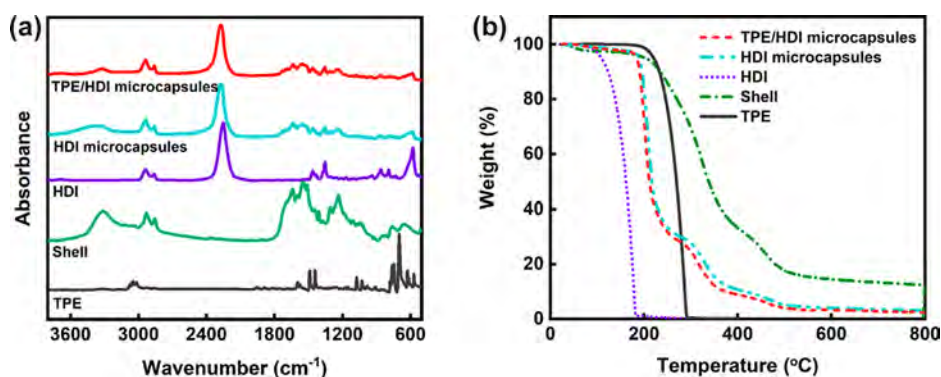


**Figure 2.** (a) FTIR spectra and (b) TGA curves of TPE/HDI microcapsules, HDI microcapsules, pure HDI, shell, and pure TPE.

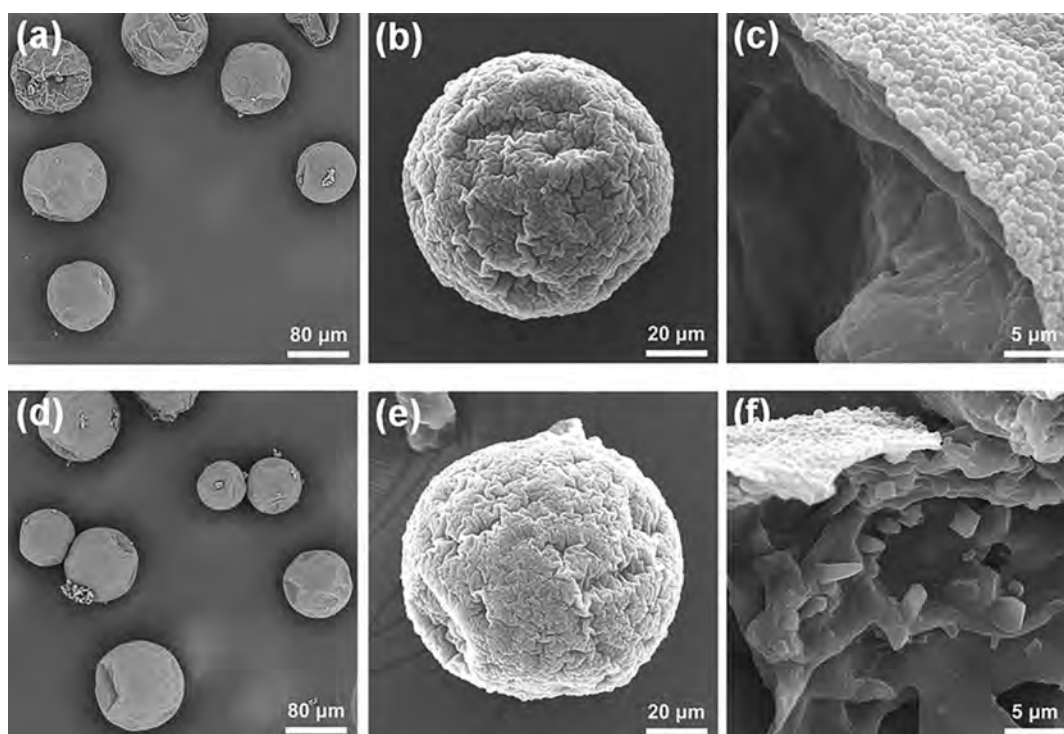


**Figure 3.** SEM images of intact microcapsules containing (a and b) HDI and (d and e) TPE/HDI, and a ruptured microcapsule containing (c) HDI and (f) TPE/HDI.

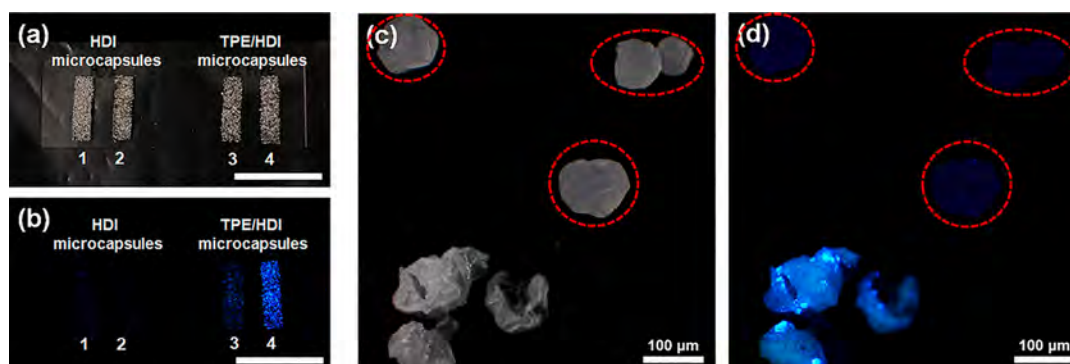


**Figure 4.** (a and b) Photographs of HDI microcapsules and TPE/HDI microcapsules taken under the illumination of (a) white light and (b) UV light. The microcapsules on strips no. 1 and no. 3 are intact, whereas those on strips no. 2 and no. 4 are ruptured. The white scale bar indicates 25 mm in both images. (c and d) Micrographs of TPE/HDI microcapsules taken under the illumination of (c) white light and (d) UV light.

the high thermal stability of their double-layer PU/PUF shells with a high initial decomposition temperature of 220 °C.

Although TPE starts to decompose at a temperature above 200 °C, it has little influence on the thermal stability of the

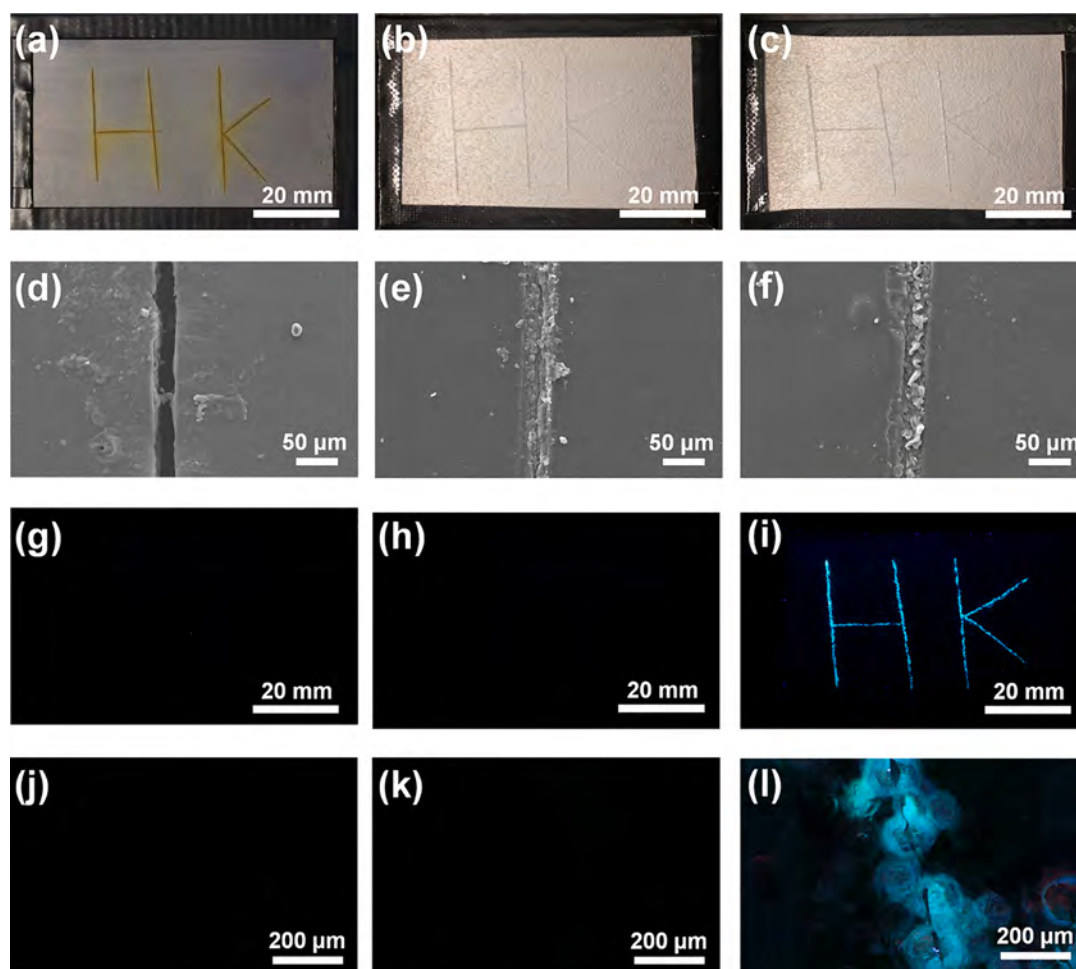


**Figure 5.** (a–c) Photographs of steel panels coated with (a) pure E-epoxy coating, (b) HDI microcapsule-embedded E-epoxy coating, and (c) TPE/HDI microcapsules-embedded E-epoxy coating taken under the illumination of white light. (d–f) SEM images of the scratched regions of (d) pure E-epoxy coating, (e) HDI microcapsule-embedded E-epoxy coating, and (f) TPE/HDI microcapsule-embedded E-epoxy coating. (g–i) Photographs of steel panels coated with (g) pure E-epoxy coating, (h) HDI microcapsule-embedded E-epoxy coating, and (i) TPE/HDI microcapsule-embedded E-epoxy coating taken under the illumination of UV light. (j–l) Micrographs of the scratched regions of (j) pure E-epoxy coating, (k) HDI microcapsule-embedded E-epoxy coating, and (l) TPE/HDI microcapsule-embedded E-epoxy coating taken using an optical microscope under the illumination of UV light.

corresponding TPE/HDI microcapsules, possibly because of its low concentration.

SEM was carried out to characterize the morphologies of the obtained microcapsules. As presented in Figure 3, both HDI and TPE/HDI microcapsules are nearly spherical with some wrinkles on the surfaces. These wrinkles are caused by the interaction of inhomogeneous reaction kinetics, shell-determined elastic forces, and fluid-induced shear forces.<sup>10</sup> Figure 3c,f suggest that the microcapsules are composed of obvious core–shell structures and their outer surfaces were deposited by a layer of PUF nanoparticles.<sup>37</sup> It is worth nothing that the ruptured HDI microcapsule shows a smooth cured inner surface. Contrary to that, many small particles are observed in the cured inner surface of the ruptured TPE/HDI microcapsules, which should be the precipitated TPE crystals.

For evaluation of the damage-reporting capability of TPE/HDI microcapsules, a few HDI and TPE/HDI microcapsules were spread on glass slides (Figure 4a, strips no. 1 and no. 3), some of which were manually damaged (Figure 4a, strips no. 2 and no. 4). There is little difference between the pure HDI microcapsule specimens and the TPE/HDI microcapsules before and after being damaged under the illumination of

white light. However, under the illumination of 365 nm UV light from a handheld UV lamp, only the ruptured TPE/HDI microcapsules exhibit strong blue fluorescence, whereas the intact HDI and TPE/HDI microcapsules and the damaged HDI microcapsules are almost nonfluorescent (Figure 4b). These results were further confirmed by the micrographs taken by an optical microscope in a single microcapsule level. Figure 4c,d shows that strong blue luminescence can be detected for damaged TPE/HDI microcapsules under UV light illumination, in contrast to the invisibility of the original microcapsules. These results imply that TPE/HDI microcapsules are promising for use in the visualization of mechanical damage. Considering the damage-reporting ability and the inherent self-healing ability of the TPE/HDI microcapsules, they show potential for application in polymer coatings with dual functions.

**3.3. Application of Dual-Function AIEgens/HDI Microcapsules in Polymer Coating.** For investigation of the autonomous self-healing and self-reporting capabilities of TPE/HDI microcapsules in polymer coating, TPE/HDI microcapsules were integrated into epoxy resin (Epilam 5015, E-epoxy). Steel panels coated with the TPE/HDI microcapsule-embedded E-epoxy coating, HDI microcapsule-embedded E-



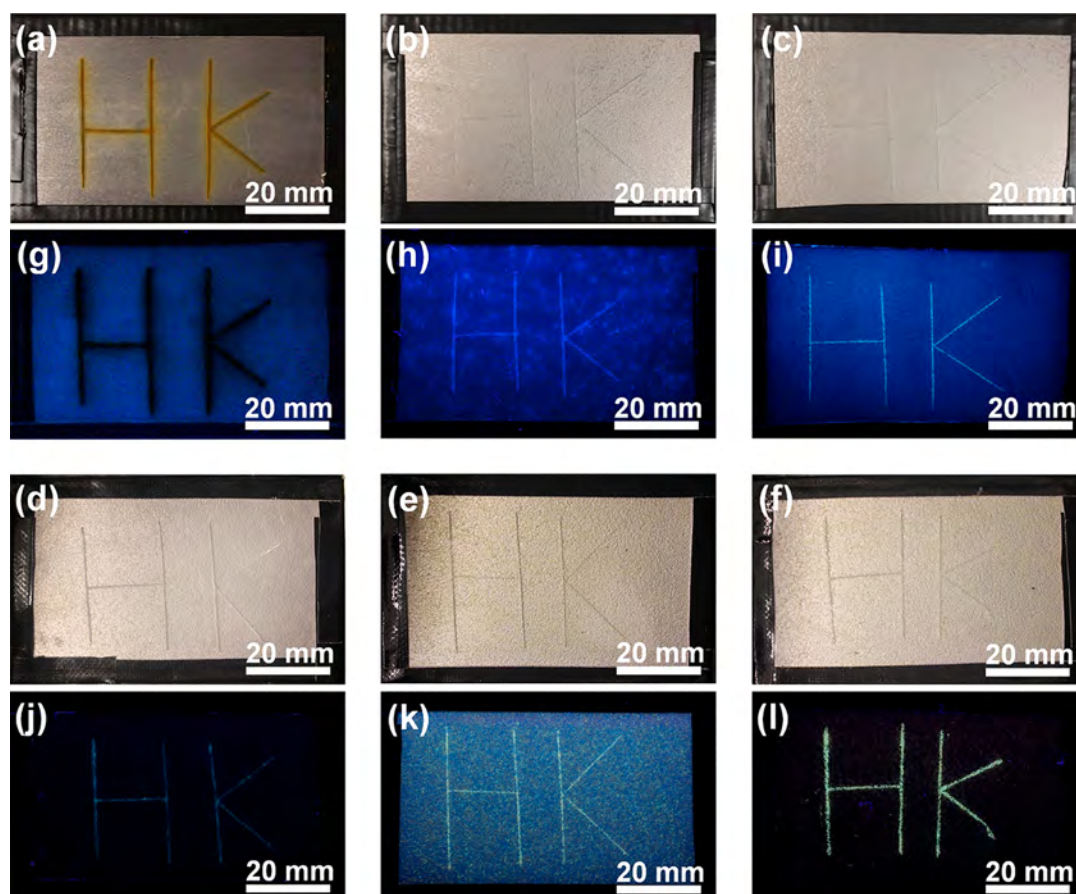


**Figure 6.** Photographs of steel panels coated with (a and g) pure S-epoxy coating, (b and h) HDI microcapsule-embedded S-epoxy coating, (c and i) TPE/HDI microcapsule-embedded S-epoxy coating, (d and j) TPE/HDI microcapsule-embedded E-epoxy coating, (e and k) DM-TPE-BMO/HDI microcapsule-embedded S-epoxy coating, and (f and l) DM-TPE-BMO/HDI microcapsule-embedded E-epoxy coating taken under the illumination of (a–f) white light and (g–l) UV light. TPE/HDI microcapsules were prepared using (a–c and g–i) 0.5 wt % and (d and j) 0.05 wt % of TPE. DM-TPE-BMO/HDI microcapsules were prepared using 0.05 wt % of DM-TPE-BMO.

epoxy coating, and pure E-epoxy coating were prepared and then scratched with a razor blade. The samples were then immersed in 10 wt % NaCl aqueous solution at room temperature for 24 h. As depicted in Figure 5a–c, the scratched regions of the steel plate coated with pure E-epoxy coating are severely corroded. By contrast, the steel plates coated with the HDI and TPE/HDI microcapsule-embedded E-epoxy coatings are almost free of rust. This observation indicates that both the HDI and TPE/HDI microcapsules endow the corresponding E-epoxy coatings with excellent corrosion protection capability for the steel panels. The SEM images (Figure 5d–f) reveal that the cracks of the HDI and TPE/HDI microcapsule-containing coatings are filled and sealed by newly formed materials. Therefore, they are capable of impeding the penetration of brine and retarding the corrosion process. Notably, the self-healing process of the E-epoxy coatings with HDI and TPE/HDI microcapsules were completely spontaneous and free of catalyst or external intervention. In addition to the self-healing ability, the fluorescent photos shown in Figure 5g–i demonstrate excellent self-reporting capability. Under the illumination of UV light, the E-epoxy coating with TPE/HDI microcapsules exhibits high-contrast visualized indication of the healed scratches, which is not observed in the control samples (pure E-epoxy coating and HDI microcapsule-embedded coating). The micrographs of the repaired scratched areas taken under UV light illumination further verified that the brilliant blue fluorescence results from

the broken TPE/HDI microcapsules in the E-epoxy coating. These results clearly demonstrate the excellent performance of the TPE/HDI microcapsule-based polymer coating with dual functions of autonomous self-healing and self-reporting.

As microcapsule-embedded coatings could be used in various practical applications, AIEgens should be not only matched with different polymer matrixes but also used in an economical fashion. In our work, a lower-cost industrial epoxy resin (Sikafloor 156, S-epoxy) was mixed with microcapsules to create functional coatings. The results depicted in Figure 6a–c and 6g–i suggested that the TPE/HDI microcapsule-embedded S-epoxy coating also shows autonomous self-healing and self-reporting dual functions. Different from the E-epoxy coating, the S-epoxy matrix was found to show blue autoluminescence. Besides S-epoxy, some other commonly used polymers have also been reported to exhibit intrinsic blue fluorescence.<sup>38–43</sup> The blue autofluorescence of the polymer matrix leads to the relatively decreased distinction between the damaged and intact areas because TPE is also blue emissive. In addition, we tried to decrease the amount of TPE used in the microcapsule preparation to make this strategy more economical. As shown in Figure 6j, however, a steel panel coated with TPE/HDI microcapsule-embedded E-epoxy coating using 0.05 wt % of TPE displays too weak fluorescence to be recognized in repaired areas. To solve these issues, a yellow emissive AIEgen (DM-TPE-BMO, a TPE derivative) with highly efficient solid-state

fluorescence was selected to replace TPE.<sup>44</sup> The chemical structure and absorption spectrum of DM-TPE-BMO are provided in Figure S4a. Similar to TPE, DM-TPE-BMO shows very faint fluorescence in its HDI solution ( $\Phi_F = 2.2\%$ ) but became strongly emissive in PU solid because of its AIE characteristic (Figure S4b). The difference is that the fluorescence of DM-TPE-BMO/PU ( $\Phi_F = 46.4\%$ ) is more efficient than that of TPE/PU ( $\Phi_F = 25.1\%$ ) and the emission maximum peaked at 531 nm. According to the aforementioned experimental procedures, DM-TPE-BMO/HDI microcapsules were successfully prepared and well characterized using 0.05 wt % of DM-TPE-BMO (Figure S5). These microcapsules were then embedded into two epoxy matrixes before being coated on steel panels to evaluate their self-reporting performance. As shown in Figure 6k,l, compared with the TPE/HDI microcapsule-embedded S-epoxy coating, the S-epoxy coating containing DM-TPE-BMO/HDI microcapsules exhibits adequate contrast between scratches and original regions. Furthermore, because of the highly efficient solid-state fluorescence of DM-TPE-BMO, the presence of merely 0.05 wt % of DM-TPE-BMO in microcapsule cores can achieve a clear observation in the healed regions of the E-epoxy coating, which is hard to observe in the E-epoxy coating containing TPE/HDI microcapsules with the same concentration of TPE.

## 4. CONCLUSION

In summary, smart coatings with autonomous self-healing and self-reporting functions were achieved by simply incorporating microcapsules that contain the HDI solution of AIEgens. When the coating is damaged, the payloads of microcapsules will be released into the cracks, which will immediately initiate the self-repairing and self-sensing progress of the core materials based on the spontaneous reaction between HDI and water as well as the restriction of intramolecular motions working mechanism of AIEgens. The photographs, SEM images, and micrographs confirmed that AIEgen/HDI microcapsule-embedded coatings were able to autonomously repair and make it conspicuous. The results using commercially available AIEgens (TPE and DM-TPE-BMO) demonstrated that the present strategy shows promise for use in diverse polymer matrixes and the content of AIEgens can even be lowered to 0.05 wt %. This facile, economical, and feasible method provides a new pathway to prepare smart anticorrosion coatings that are of great interest to the industrial field.

## ■ ASSOCIATED CONTENT

### Supporting Information

The Supporting Information is available free of charge at <https://pubs.acs.org/doi/10.1021/acsami.9b18919>.

UV-vis absorption spectra of TPE/HDI, TPE/THF, DM-TPE-BMO/HDI, and DM-TPE-BMO/THF solution; PL spectra of DM-TPE-BMO/HDI solution and DM-TPE-BMO/PU solid; calculation method for the core fraction of microcapsules; typical isothermal TGA curves of HDI microcapsules and shell; size distributions, diameter, and core fraction of microcapsules as a function of agitation rate for PU synthesis; core fraction of microcapsules as a function of reaction duration for PUF synthesis; FTIR spectra of DM-TPE-BMO/HDI microcapsules and pure DM-TPE-BMO; TGA curves of DM-TPE-BMO/HDI microcapsules and pure DM-TPE-BMO; photographs of intact DM-TPE-BMO/HDI

microcapsules and ruptured DM-TPE-BMO/HDI microcapsules taken under the illumination of white light and UV light, respectively; micrographs of DM-TPE-BMO/HDI microcapsules taken under the illumination of white light and UV light, respectively (PDF)

## ■ AUTHOR INFORMATION

### Corresponding Authors

**Ben Zhong Tang** – Shenzhen University, Shenzhen, China, and The Hong Kong University of Science and Technology, Clear Water Bay, Hong Kong SAR, China; [orcid.org/0000-0002-0293-964X](https://orcid.org/0000-0002-0293-964X); Email: [tangbenz@ust.hk](mailto:tangbenz@ust.hk)

**Jinglei Yang** – The Hong Kong University of Science and Technology, Clear Water Bay, Hong Kong SAR, China; [orcid.org/0000-0002-9413-9016](https://orcid.org/0000-0002-9413-9016); Email: [maeyang@ust.hk](mailto:maeyang@ust.hk)

### Other Authors

**Shusheng Chen** – The Hong Kong University of Science and Technology, Clear Water Bay, Hong Kong SAR, China; [orcid.org/0000-0002-3010-7963](https://orcid.org/0000-0002-3010-7963)

**Ting Han** – Shenzhen University, Shenzhen, China, and The Hong Kong University of Science and Technology, Clear Water Bay, Hong Kong SAR, China; [orcid.org/0000-0003-1521-6333](https://orcid.org/0000-0003-1521-6333)

**Ying Zhao** – The Hong Kong University of Science and Technology, Clear Water Bay, Hong Kong SAR, China

**Wenjun Luo** – The Hong Kong University of Science and Technology, Clear Water Bay, Hong Kong SAR, China

**Zhong Zhang** – National Center for Nanoscience and Technology, Beijing, China; [orcid.org/0000-0002-9102-1311](https://orcid.org/0000-0002-9102-1311)

**Haibin Su** – The Hong Kong University of Science and Technology, Clear Water Bay, Hong Kong SAR, China; [orcid.org/0000-0001-9760-6567](https://orcid.org/0000-0001-9760-6567)

Complete contact information is available at: <https://pubs.acs.org/doi/10.1021/acsami.9b18919>

### Notes

The authors declare no competing financial interest.

## ■ ACKNOWLEDGMENTS

The work was financially supported by The Hong Kong University of Science and Technology (Grant No.: R9365), NSFC/RGC Joint Research Scheme of Hong Kong (Grant No.: N\_HKUST 631/18), and Zhongshan-HKUST Program (Project ID: RG066). The authors are grateful to Graham Young from MAE of HKUST for the constructive discussion and input for this article.

## ■ REFERENCES

- (1) Zhang, P.; Li, G. Advances in healing-on-demand polymers and polymer composites. *Prog. Polym. Sci.* **2016**, *57*, 32–63.
- (2) Diesendruck, C. E.; Sottos, N. R.; Moore, J. S.; White, S. R. Biomimetic Self-Healing. *Angew. Chem., Int. Ed.* **2015**, *54*, 10428–10447.
- (3) Yang, Y.; Ding, X.; Urban, M. W. Chemical and physical aspects of self-healing materials. *Prog. Polym. Sci.* **2015**, *49–50*, 34–59.
- (4) White, S. R.; Sottos, N. R.; Geubelle, P. H.; Moore, J. S.; Kessler, M. R.; Sriram, S. R.; Brown, E. N.; Viswanathan, S. Autonomic healing of polymer composites. *Nature* **2001**, *409*, 794–797.



- (5) Rule, J. D.; Sottos, N. R.; White, S. R. Effect of microcapsule size on the performance of self-healing polymers. *Polymer* **2007**, *48*, 3520–3529.
- (6) Coope, T. S.; Mayer, U. F. J.; Wass, D. F.; Trask, R. S.; Bond, I. P. Self-Healing of an Epoxy Resin Using Scandium(III) Triflate as a Catalytic Curing Agent. *Adv. Funct. Mater.* **2011**, *21*, 4624–4631.
- (7) Zhang, H.; Zhang, X.; Bao, C.; Li, X.; Sun, D.; Duan, F.; Friedrich, K.; Yang, J. Direct microencapsulation of pure polyamine by integrating microfluidic emulsion and interfacial polymerization for practical self-healing materials. *J. Mater. Chem. A* **2018**, *6*, 24092–24099.
- (8) Yuan, Y. C.; Ye, X. J.; Rong, M. Z.; Zhang, M. Q.; Yang, G. C.; Zhao, J. Q. Self-healing epoxy composite with heat-resistant healant. *ACS Appl. Mater. Interfaces* **2011**, *3*, 4487–4495.
- (9) Meng, L. M.; Yuan, Y. C.; Rong, M. Z.; Zhang, M. Q. A dual mechanism single-component self-healing strategy for polymers. *J. Mater. Chem.* **2010**, *20*, 6030–6038.
- (10) Yang, J.; Keller, M. W.; Moore, J. S.; White, S. R.; Sottos, N. R. Microencapsulation of Isocyanates for Self-Healing Polymers. *Macromolecules* **2008**, *41*, 9650–9655.
- (11) Zhu, D. Y.; Rong, M. Z.; Zhang, M. Q. Self-healing polymeric materials based on microencapsulated healing agents: From design to preparation. *Prog. Polym. Sci.* **2015**, *49*, 175–220.
- (12) Calvino, C.; Weder, C. Microcapsule-Containing Self-Reporting Polymers. *Small* **2018**, *14*, 1802489.
- (13) Postiglione, G.; Colombo, A.; Dragonetti, C.; Levi, M.; Turri, S.; Griffini, G. Fluorescent probes based on chemically-stable core/shell microcapsules for visual microcrack detection. *Sens. Actuators, B* **2017**, *248*, 35–42.
- (14) Song, Y.-K.; Lee, K.-H.; Kim, D.-M.; Chung, C.-M. A microcapsule-type fluorescent probe for the detection of microcracks in cementitious materials. *Sens. Actuators, B* **2016**, *222*, 1159–1165.
- (15) Di Credico, B.; Griffini, G.; Levi, M.; Turri, S. Microencapsulation of a UV-responsive photochromic dye by means of novel UV-screening polyurea-based shells for smart coating applications. *ACS Appl. Mater. Interfaces* **2013**, *5*, 6628–6634.
- (16) Li, W.; Matthews, C. C.; Yang, K.; Odarczenko, M. T.; White, S. R.; Sottos, N. R. Autonomous Indication of Mechanical Damage in Polymeric Coatings. *Adv. Mater.* **2016**, *28*, 2189–2194.
- (17) Vidinejevs, S.; Aniskevich, A. N.; Gregor, A.; Sjöberg, M.; Alvarez, G. Smart polymeric coatings for damage visualization in substrate materials. *J. Intell. Mater. Syst. Struct.* **2012**, *23*, 1371–1377.
- (18) Odom, S. A.; Jackson, A. C.; Prokup, A. M.; Chayanupatkul, S.; Sottos, N. R.; White, S. R.; Moore, J. S. Visual indication of mechanical damage using core-shell microcapsules. *ACS Appl. Mater. Interfaces* **2011**, *3*, 4547–4551.
- (19) van den Dungen, E. T. A.; Loos, B.; Klumperman, B. Use of a profluorophore for visualization of the rupture of capsules in self-healing coatings. *Macromol. Rapid Commun.* **2010**, *31*, 625–628.
- (20) Döhler, D.; Rana, S.; Rupp, H.; Bergmann, H.; Behzadi, S.; Crespy, D.; Binder, W. H. Qualitative sensing of mechanical damage by a fluorogenic “click” reaction. *Chem. Commun.* **2016**, *52*, 11076–11079.
- (21) Lavrenova, A.; Farkas, J.; Weder, C.; Simon, Y. C. Visualization of Polymer Deformation Using Microcapsules Filled with Charge-Transfer Complex Precursors. *ACS Appl. Mater. Interfaces* **2015**, *7*, 21828–21834.
- (22) Calvino, C.; Guha, A.; Weder, C.; Schrettl, S. Self-Calibrating Mechanochromic Fluorescent Polymers Based on Encapsulated Excimer-Forming Dyes. *Adv. Mater.* **2018**, *30*, 1704603.
- (23) Lee, T. H.; Song, Y. K.; Park, S. H.; Park, Y. I.; Noh, S. M.; Kim, J. C. Dual stimuli responsive self-reporting material for chemical reservoir coating. *Appl. Surf. Sci.* **2018**, *434*, 1327–1335.
- (24) Lu, X.; Li, W.; Sottos, N. R.; Moore, J. S. Autonomous Damage Detection in Multilayered Coatings via Integrated Aggregation-Induced Emission Luminogens. *ACS Appl. Mater. Interfaces* **2018**, *10*, 40361–40365.
- (25) Robb, M. J.; Li, W.; Gergely, R. C. R.; Matthews, C. C.; White, S. R.; Sottos, N. R.; Moore, J. S. A Robust Damage-Reporting Strategy for Polymeric Materials Enabled by Aggregation-Induced Emission. *ACS Cent. Sci.* **2016**, *2*, 598–603.
- (26) Zhang, H.; Zhang, X.; Bao, C.; Li, X.; Duan, F.; Friedrich, K.; Yang, J. Skin-Inspired, Fully Autonomous Self-Warning and Self-Repairing Polymeric Material under Damaging Events. *Chem. Mater.* **2019**, *31*, 2611–2618.
- (27) Wang, J.-P.; Wang, J.-K.; Zhou, Q.; Li, Z.; Han, Y.; Song, Y.; Yang, S.; Song, X.; Qi, T.; Möhwalld, H. Adaptive Polymeric Coatings with Self-Reporting and Self-Healing Dual Functions from Porous Core-Shell Nanostructures. *Macromol. Mater. Eng.* **2018**, *303*, 1700616.
- (28) Hu, M.; Peil, S.; Xing, Y.; Döhler, D.; Caire da Silva, L.; Binder, W. H.; Kappl, M.; Bannwarth, M. B. Monitoring crack appearance and healing in coatings with damage self-reporting nanocapsules. *Mater. Horiz.* **2018**, *5*, 51–58.
- (29) Song, Y. K.; Kim, B.; Lee, T. H.; Kim, J. C.; Nam, J. H.; Noh, S. M.; Park, Y. I. Fluorescence Detection of Microcapsule-Type Self-Healing, Based on Aggregation-Induced Emission. *Macromol. Rapid Commun.* **2017**, *38*, 1600657.
- (30) Song, Y. K.; Kim, B.; Lee, T. H.; Kim, S. Y.; Kim, J. C.; Noh, S. M.; Park, Y. I. Monitoring Fluorescence Colors to Separately Identify Cracks and Healed Cracks in Microcapsule-containing Self-healing Coating. *Sens. Actuators, B* **2018**, *257*, 1001–1008.
- (31) Huang, M.; Yang, J. Facile microencapsulation of HDI for self-healing anticorrosion coatings. *J. Mater. Chem.* **2011**, *21*, 11123–11130.
- (32) Wu, G.; An, J.; Sun, D.; Tang, X.; Xiang, Y.; Yang, J. Robust microcapsules with polyurea/silica hybrid shell for one-part self-healing anticorrosion coatings. *J. Mater. Chem. A* **2014**, *2*, 11614–11620.
- (33) Sun, D.; An, J.; Wu, G.; Yang, J. Double-layered reactive microcapsules with excellent thermal and non-polar solvent resistance for self-healing coatings. *J. Mater. Chem. A* **2015**, *3*, 4435–4444.
- (34) Sun, D.; Zhang, H.; Tang, X.-Z.; Yang, J. Water resistant reactive microcapsules for self-healing coatings in harsh environments. *Polymer* **2016**, *91*, 33–40.
- (35) Sun, D.; Chong, Y. B.; Chen, K.; Yang, J. Chemically and thermally stable isocyanate microcapsules having good self-healing and self-lubricating performances. *Chem. Eng. J.* **2018**, *346*, 289–297.
- (36) Shi, J.; Chang, N.; Li, C.; Mei, J.; Deng, C.; Luo, X.; Liu, Z.; Bo, Z.; Dong, Y. Q.; Tang, B. Z. Locking the phenyl rings of tetraphenylethene step by step: Understanding the mechanism of aggregation-induced emission. *Chem. Commun.* **2012**, *48*, 10675–10677.
- (37) Brown, E. N.; Kessler, M. R.; Sottos, N. R.; White, S. R. In situ poly(urea-formaldehyde) microencapsulation of dicyclopentadiene. *J. Microencapsulation* **2003**, *20*, 719–730.
- (38) Zhang Yuan, W.; Zhang, Y. Nonconventional macromolecular luminogens with aggregation-induced emission characteristics. *J. Polym. Sci., Part A: Polym. Chem.* **2017**, *55*, S60–S74.
- (39) Zhou, X.; Luo, W.; Nie, H.; Xu, L.; Hu, R.; Zhao, Z.; Qin, A.; Tang, B. Z. Oligo(maleic anhydride)s: A platform for unveiling the mechanism of clusteroluminescence of non-aromatic polymers. *J. Mater. Chem. C* **2017**, *5*, 4775–4779.
- (40) Zhao, E.; Lam, J. W. Y.; Meng, L.; Hong, Y.; Deng, H.; Bai, G.; Huang, X.; Hao, J.; Tang, B. Z. Poly[(maleic anhydride)-alt-(vinyl acetate)]: A Pure Oxygenic Nonconjugated Macromolecule with Strong Light Emission and Solvatochromic Effect. *Macromolecules* **2015**, *48*, 64–71.
- (41) Li, K.; Lin, Y.; Lu, C. Aggregation-Induced Emission for Visualization in Materials Science. *Chem. - Asian J.* **2019**, *14*, 715–729.
- (42) Mei, J.; Leung, N. L. C.; Kwok, R. T. K.; Lam, J. W. Y.; Tang, B. Z. Aggregation-Induced Emission: Together We Shine, United We Soar! *Chem. Rev.* **2015**, *115*, 11718–11940.
- (43) Wu, D.; Sedgwick, A. C.; Gunnlaugsson, T.; Akkaya, E. U.; Yoon, J.; James, T. D. Fluorescent chemosensors: The past, present and future. *Chem. Soc. Rev.* **2017**, *46*, 7105–7123.
- (44) Zhang, Y.; Jiang, M.; Han, T.; Xiao, X.; Chen, W.; Wang, L.; Wong, K. S.; Wang, R.; Wang, K.; Tang, B. Z. Aggregation-Induced Emission Luminogens as Color Converters for Visible-Light Communication. *ACS Appl. Mater. Interfaces* **2018**, *10*, 34418–34426.